

## Azimuthal-Angle Dependence of Charged-Pion-Interferometry Measurements with Respect to Second- and Third-Order Event Planes in Au + Au Collisions at $\sqrt{s_{NN}} = 200$ GeV

A. Adare,<sup>13</sup> S. Afanasiev,<sup>30</sup> C. Aidala,<sup>43,44</sup> N. N. Ajitanand,<sup>62</sup> Y. Akiba,<sup>56,57</sup> H. Al-Bataineh,<sup>50</sup> J. Alexander,<sup>62</sup> K. Aoki,<sup>35,56</sup> Y. Aramaki,<sup>12</sup> E. T. Atomssa,<sup>36</sup> R. Averbeck,<sup>63</sup> T. C. Awes,<sup>52</sup> B. Azmoun,<sup>7</sup> V. Babintsev,<sup>24</sup> M. Bai,<sup>6</sup> G. Baksay,<sup>20</sup> L. Baksay,<sup>20</sup> K. N. Barish,<sup>8</sup> B. Bassalleck,<sup>49</sup> A. T. Basye,<sup>1</sup> S. Bathe,<sup>5,8</sup> V. Baublis,<sup>55</sup> C. Baumann,<sup>45</sup> A. Bazilevsky,<sup>7</sup> S. Belikov,<sup>7,\*</sup> R. Belmont,<sup>67</sup> R. Bennett,<sup>63</sup> A. Berdnikov,<sup>59</sup> Y. Berdnikov,<sup>59</sup> A. A. Bickley,<sup>13</sup> J. S. Bok,<sup>71</sup> K. Boyle,<sup>63</sup> M. L. Brooks,<sup>39</sup> H. Buesching,<sup>7</sup> V. Bumazhnov,<sup>24</sup> G. Bunce,<sup>7,57</sup> S. Butsyk,<sup>39</sup> C. M. Camacho,<sup>39</sup> S. Campbell,<sup>63</sup> C.-H. Chen,<sup>63</sup> C. Y. Chi,<sup>14</sup> M. Chiu,<sup>7</sup> I. J. Choi,<sup>71</sup> R. K. Choudhury,<sup>4</sup> P. Christiansen,<sup>41</sup> T. Chujo,<sup>66</sup> P. Chung,<sup>62</sup> O. Chvala,<sup>8</sup> V. Cianciolo,<sup>52</sup> Z. Citron,<sup>63</sup> B. A. Cole,<sup>14</sup> M. Connors,<sup>63</sup> P. Constantin,<sup>39</sup> M. Csanád,<sup>18</sup> T. Csörgő,<sup>70</sup> T. Dahms,<sup>63</sup> S. Dairaku,<sup>35,56</sup> I. Danchev,<sup>67</sup> K. Das,<sup>21</sup> A. Datta,<sup>43</sup> G. David,<sup>7</sup> A. Denisov,<sup>24</sup> A. Deshpande,<sup>57,63</sup> E. J. Desmond,<sup>7</sup> O. Dietzsch,<sup>60</sup> A. Dion,<sup>63</sup> M. Donadelli,<sup>60</sup> O. Drapier,<sup>36</sup> A. Drees,<sup>63</sup> K. A. Drees,<sup>6</sup> J. M. Durham,<sup>39,63</sup> A. Durum,<sup>24</sup> D. Dutta,<sup>4</sup> S. Edwards,<sup>21</sup> Y. V. Efremenko,<sup>52</sup> F. Ellinghaus,<sup>13</sup> T. Engelmöore,<sup>14</sup> A. Enokizono,<sup>38</sup> H. En'yo,<sup>56,57</sup> S. Esumi,<sup>66</sup> B. Fadem,<sup>46</sup> D. E. Fields,<sup>49</sup> M. Finger,<sup>9</sup> M. Finger, Jr.,<sup>9</sup> F. Fleuret,<sup>36</sup> S. L. Fokin,<sup>34</sup> Z. Fraenkel,<sup>69,\*</sup> J. E. Frantz,<sup>51,63</sup> A. Franz,<sup>7</sup> A. D. Frawley,<sup>21</sup> K. Fujiwara,<sup>56</sup> Y. Fukao,<sup>56</sup> T. Fusayasu,<sup>48</sup> I. Garishvili,<sup>64</sup> A. Glenn,<sup>13</sup> H. Gong,<sup>63</sup> M. Gonin,<sup>36</sup> Y. Goto,<sup>56,57</sup> R. Granier de Cassagnac,<sup>36</sup> N. Grau,<sup>2,14</sup> S. V. Greene,<sup>67</sup> M. Grosse Perdekamp,<sup>25,57</sup> T. Gunji,<sup>12</sup> H.-Å. Gustafsson,<sup>41,\*</sup> J. S. Haggerty,<sup>7</sup> K. I. Hahn,<sup>19</sup> H. Hamagaki,<sup>12</sup> J. Hamblen,<sup>64</sup> R. Han,<sup>54</sup> J. Hanks,<sup>14</sup> E. P. Hartouni,<sup>38</sup> E. Haslum,<sup>41</sup> R. Hayano,<sup>12</sup> X. He,<sup>22</sup> M. Heffner,<sup>38</sup> T. K. Hemmick,<sup>63</sup> T. Hester,<sup>8</sup> J. C. Hill,<sup>28</sup> M. Hohlmann,<sup>20</sup> W. Holzmann,<sup>14</sup> K. Homma,<sup>23</sup> B. Hong,<sup>33</sup> T. Horaguchi,<sup>23</sup> D. Hornback,<sup>64</sup> S. Huang,<sup>67</sup> T. Ichihara,<sup>56,57</sup> R. Ichimiya,<sup>56</sup> J. Ide,<sup>46</sup> Y. Ikeda,<sup>66</sup> K. Imai,<sup>29,35,56</sup> M. Inaba,<sup>66</sup> D. Isenhower,<sup>1</sup> M. Ishihara,<sup>56</sup> T. Isobe,<sup>12,56</sup> M. Issah,<sup>67</sup> A. Isupov,<sup>30</sup> D. Ivanischev,<sup>55</sup> B. V. Jacak,<sup>63</sup> J. Jia,<sup>7,62</sup> J. Jin,<sup>14</sup> B. M. Johnson,<sup>7</sup> K. S. Joo,<sup>47</sup> D. Jouan,<sup>53</sup> D. S. Jumper,<sup>1</sup> F. Kajihara,<sup>12</sup> S. Kametani,<sup>56</sup> N. Kamihara,<sup>57</sup> J. Kamin,<sup>63</sup> J. H. Kang,<sup>71</sup> J. Kapustinsky,<sup>39</sup> K. Karatsu,<sup>35,56</sup> D. Kallow,<sup>43,57</sup> M. Kawashima,<sup>56,58</sup> A. V. Kazantsev,<sup>34</sup> T. Kempel,<sup>28</sup> A. Khanzadeev,<sup>55</sup> K. M. Kijima,<sup>23</sup> B. I. Kim,<sup>33</sup> D. H. Kim,<sup>47</sup> D. J. Kim,<sup>31</sup> E. Kim,<sup>61</sup> E.-J. Kim,<sup>10</sup> S. H. Kim,<sup>71</sup> Y.-J. Kim,<sup>25</sup> E. Kinney,<sup>13</sup> K. Kiriluk,<sup>13</sup> Á. Kiss,<sup>18</sup> E. Kistenev,<sup>7</sup> L. Kochenda,<sup>55</sup> B. Komkov,<sup>55</sup> M. Konno,<sup>66</sup> J. Koster,<sup>25</sup> D. Kotchetkov,<sup>49</sup> A. Kozlov,<sup>69</sup> A. Král,<sup>15</sup> A. Kravitz,<sup>14</sup> G. J. Kunde,<sup>39</sup> K. Kurita,<sup>56,58</sup> M. Kurosawa,<sup>56</sup> Y. Kwon,<sup>71</sup> G. S. Kyle,<sup>50</sup> R. Lacey,<sup>62</sup> Y. S. Lai,<sup>14</sup> J. G. Lajoie,<sup>28</sup> A. Lebedev,<sup>28</sup> D. M. Lee,<sup>39</sup> J. Lee,<sup>19</sup> K. Lee,<sup>61</sup> K. B. Lee,<sup>33</sup> K. S. Lee,<sup>33</sup> M. J. Leitch,<sup>39</sup> M. A. L. Leite,<sup>60</sup> E. Leitner,<sup>67</sup> B. Lenzi,<sup>60</sup> X. Li,<sup>11</sup> P. Liebing,<sup>57</sup> L. A. Linden Levy,<sup>13</sup> T. Liška,<sup>15</sup> A. Litvinenko,<sup>30</sup> H. Liu,<sup>39,50</sup> M. X. Liu,<sup>39</sup> B. Love,<sup>67</sup> R. Luechtenborg,<sup>45</sup> D. Lynch,<sup>7</sup> C. F. Maguire,<sup>67</sup> Y. I. Makdisi,<sup>6</sup> A. Malakhov,<sup>30</sup> M. D. Malik,<sup>49</sup> V. I. Manko,<sup>34</sup> E. Mannel,<sup>14</sup> Y. Mao,<sup>54,56</sup> H. Masui,<sup>66</sup> F. Matathias,<sup>14</sup> M. McCumber,<sup>63</sup> P. L. McGaughey,<sup>39</sup> N. Means,<sup>63</sup> B. Meredith,<sup>25</sup> Y. Miake,<sup>66</sup> A. C. Mignerey,<sup>42</sup> P. Mikeš,<sup>9,27</sup> K. Miki,<sup>56,66</sup> A. Milov,<sup>7</sup> M. Mishra,<sup>3</sup> J. T. Mitchell,<sup>7</sup> A. K. Mohanty,<sup>4</sup> Y. Morino,<sup>12</sup> A. Morreale,<sup>8</sup> D. P. Morrison,<sup>7,†</sup> T. V. Moukhanova,<sup>34</sup> J. Murata,<sup>56,58</sup> S. Nagamiya,<sup>32</sup> J. L. Nagle,<sup>13,‡</sup> M. Naglis,<sup>69</sup> M. I. Nagy,<sup>18</sup> I. Nakagawa,<sup>56,57</sup> Y. Nakamiya,<sup>23</sup> T. Nakamura,<sup>32</sup> K. Nakano,<sup>56,65</sup> J. Newby,<sup>38</sup> M. Nguyen,<sup>63</sup> T. Niida,<sup>66</sup> R. Nouicer,<sup>7</sup> A. S. Nyanin,<sup>34</sup> E. O'Brien,<sup>7</sup> S. X. Oda,<sup>12</sup> C. A. Ogilvie,<sup>28</sup> M. Oka,<sup>66</sup> K. Okada,<sup>57</sup> Y. Onuki,<sup>56</sup> A. Oskarsson,<sup>41</sup> M. Ouchida,<sup>23,56</sup> K. Ozawa,<sup>12</sup> R. Pak,<sup>7</sup> V. Pantuev,<sup>26,63</sup> V. Papavassiliou,<sup>50</sup> I. H. Park,<sup>19</sup> J. Park,<sup>61</sup> S. K. Park,<sup>33</sup> W. J. Park,<sup>33</sup> S. F. Pate,<sup>50</sup> H. Pei,<sup>28</sup> J.-C. Peng,<sup>25</sup> H. Pereira,<sup>16</sup> V. Peresedov,<sup>30</sup> D. Yu. Peressouko,<sup>34</sup> C. Pinkenburg,<sup>7</sup> R. P. Pisani,<sup>7</sup> M. Proissl,<sup>63</sup> M. L. Purschke,<sup>7</sup> A. K. Purwar,<sup>39</sup> H. Qu,<sup>22</sup> J. Rak,<sup>31</sup> A. Rakotozafindrabe,<sup>36</sup> I. Ravinovich,<sup>69</sup> K. F. Read,<sup>52,64</sup> K. Reygers,<sup>45</sup> V. Riabov,<sup>55</sup> Y. Riabov,<sup>55</sup> E. Richardson,<sup>42</sup> D. Roach,<sup>67</sup> G. Roche,<sup>40</sup> S. D. Rolnick,<sup>8</sup> M. Rosati,<sup>28</sup> C. A. Rosen,<sup>13</sup> S. S. E. Rosendahl,<sup>41</sup> P. Rosnet,<sup>40</sup> P. Rukoyatkin,<sup>30</sup> P. Ružička,<sup>27</sup> B. Sahlmueller,<sup>45,63</sup> N. Saito,<sup>32</sup> T. Sakaguchi,<sup>7</sup> K. Sakashita,<sup>56,65</sup> V. Samsonov,<sup>55</sup> S. Sano,<sup>12,68</sup> T. Sato,<sup>66</sup> S. Sawada,<sup>32</sup> K. Sedgwick,<sup>8</sup> J. Seele,<sup>13</sup> R. Seidl,<sup>25</sup> A. Yu. Semenov,<sup>28</sup> R. Seto,<sup>8</sup> D. Sharma,<sup>69</sup> I. Shein,<sup>24</sup> T.-A. Shibata,<sup>56,65</sup> K. Shigaki,<sup>23</sup> M. Shimomura,<sup>66</sup> K. Shoji,<sup>35,56</sup> P. Shukla,<sup>4</sup> A. Sickles,<sup>7</sup> C. L. Silva,<sup>60</sup> D. Silvermyr,<sup>52</sup> C. Silvestre,<sup>16</sup> K. S. Sim,<sup>33</sup> B. K. Singh,<sup>3</sup> C. P. Singh,<sup>3</sup> V. Singh,<sup>3</sup> M. Slunečka,<sup>9</sup> R. A. Soltz,<sup>38</sup> W. E. Sondheim,<sup>39</sup> S. P. Sorensen,<sup>64</sup> I. V. Sourikova,<sup>7</sup> N. A. Sparks,<sup>1</sup> P. W. Stankus,<sup>52</sup> E. Stenlund,<sup>41</sup> S. P. Stoll,<sup>7</sup> T. Sugitate,<sup>23</sup> A. Sukhanov,<sup>7</sup> J. Sziklai,<sup>70</sup> E. M. Takagui,<sup>60</sup> A. Taketani,<sup>56,57</sup> R. Tanabe,<sup>66</sup> Y. Tanaka,<sup>48</sup> K. Tanida,<sup>35,56,57</sup> M. J. Tannenbaum,<sup>7</sup> S. Tarafdar,<sup>3</sup> A. Taranenko,<sup>62</sup> P. Tarján,<sup>17</sup> H. Themann,<sup>63</sup> T. L. Thomas,<sup>49</sup> T. Todoroki,<sup>56,66</sup> M. Togawa,<sup>35,56</sup> A. Toia,<sup>63</sup> L. Tomášek,<sup>27</sup> H. Torii,<sup>23</sup> R. S. Towell,<sup>1</sup> I. Tseruya,<sup>69</sup> Y. Tsuchimoto,<sup>23</sup> C. Vale,<sup>7,28</sup> H. Valle,<sup>67</sup> H. W. van Hecke,<sup>39</sup> E. Vazquez-Zambrano,<sup>14</sup> A. Veicht,<sup>25</sup> J. Velkovska,<sup>67</sup> R. Vértesi,<sup>17,70</sup> A. A. Vinogradov,<sup>34</sup> M. Virius,<sup>15</sup> V. Vrba,<sup>27</sup> E. Vznuzdaev,<sup>55</sup> X. R. Wang,<sup>50</sup> D. Watanabe,<sup>23</sup> K. Watanabe,<sup>66</sup> Y. Watanabe,<sup>56,57</sup> F. Wei,<sup>28</sup> R. Wei,<sup>62</sup> J. Wessels,<sup>45</sup> S. N. White,<sup>7</sup> D. Winter,<sup>14</sup> J. P. Wood,<sup>1</sup> C. L. Woody,<sup>7</sup> R. M. Wright,<sup>1</sup> M. Wysocki,<sup>13</sup> W. Xie,<sup>57</sup> Y. L. Yamaguchi,<sup>12</sup> K. Yamaura,<sup>23</sup> R. Yang,<sup>25</sup> A. Yanovich,<sup>24</sup>

J. Ying,<sup>22</sup> S. Yokkaichi,<sup>56,57</sup> Z. You,<sup>54</sup> G. R. Young,<sup>52</sup> I. Younus,<sup>37,49</sup> I. E. Yushmanov,<sup>34</sup> W. A. Zajc,<sup>14</sup> C. Zhang,<sup>52</sup>  
S. Zhou,<sup>11</sup> and L. Zolin<sup>30</sup>

(PHENIX Collaboration)

- <sup>1</sup>Abilene Christian University, Abilene, Texas 79699, USA  
<sup>2</sup>Department of Physics, Augustana College, Sioux Falls, South Dakota 57197, USA  
<sup>3</sup>Department of Physics, Banaras Hindu University, Varanasi 221005, India  
<sup>4</sup>Bhabha Atomic Research Centre, Bombay 400 085, India  
<sup>5</sup>Baruch College, City University of New York, New York, New York 10010 USA  
<sup>6</sup>Collider-Accelerator Department, Brookhaven National Laboratory, Upton, New York 11973-5000, USA  
<sup>7</sup>Physics Department, Brookhaven National Laboratory, Upton, New York 11973-5000, USA  
<sup>8</sup>University of California—Riverside, Riverside, California 92521, USA  
<sup>9</sup>Charles University, Ovocný trh 5, Praha 1, 116 36, Prague, Czech Republic  
<sup>10</sup>Chonbuk National University, Jeonju, 561-756, Korea  
<sup>11</sup>Science and Technology on Nuclear Data Laboratory, China Institute of Atomic Energy, Beijing 102413, People's Republic of China  
<sup>12</sup>Center for Nuclear Study, Graduate School of Science, University of Tokyo, 7-3-1 Hongo, Bunkyo, Tokyo 113-0033, Japan  
<sup>13</sup>University of Colorado, Boulder, Colorado 80309, USA  
<sup>14</sup>Columbia University, New York, New York 10027, USA and Nevis Laboratories, Irvington, New York 10533, USA  
<sup>15</sup>Czech Technical University, Zikova 4, 166 36 Prague 6, Czech Republic  
<sup>16</sup>Dapnia, CEA Saclay, F-91191, Gif-sur-Yvette, France  
<sup>17</sup>Debrecen University, H-4010 Debrecen, Egyetem tér 1, Hungary  
<sup>18</sup>ELTE, Eötvös Loránd University, H-1117 Budapest, Pázmány Péter sétány 1/A, Hungary  
<sup>19</sup>Ewha Womans University, Seoul 120-750, Korea  
<sup>20</sup>Florida Institute of Technology, Melbourne, Florida 32901, USA  
<sup>21</sup>Florida State University, Tallahassee, Florida 32306, USA  
<sup>22</sup>Georgia State University, Atlanta, Georgia 30303, USA  
<sup>23</sup>Hiroshima University, Kagamiyama, Higashi-Hiroshima 739-8526, Japan  
<sup>24</sup>IHEP Protvino, State Research Center of Russian Federation, Institute for High Energy Physics, Protvino 142281, Russia  
<sup>25</sup>University of Illinois at Urbana-Champaign, Urbana, Illinois 61801, USA  
<sup>26</sup>Institute for Nuclear Research of the Russian Academy of Sciences, Prospekt 60-letiya Oktyabrya 7a, Moscow 117312, Russia  
<sup>27</sup>Institute of Physics, Academy of Sciences of the Czech Republic, Na Slovance 2, 182 21 Prague 8, Czech Republic  
<sup>28</sup>Iowa State University, Ames, Iowa 50011, USA  
<sup>29</sup>Advanced Science Research Center, Japan Atomic Energy Agency, 2-4 Shirakata Shirane, Tokai-mura, Naka-gun, Ibaraki-ken 319-1195, Japan  
<sup>30</sup>Joint Institute for Nuclear Research, 141980 Dubna, Moscow Region, Russia  
<sup>31</sup>Helsinki Institute of Physics and University of Jyväskylä, P.O. Box 35, FI-40014 Jyväskylä, Finland  
<sup>32</sup>KEK, High Energy Accelerator Research Organization, Tsukuba, Ibaraki 305-0801, Japan  
<sup>33</sup>Korea University, Seoul, 136-701, Korea  
<sup>34</sup>Russian Research Center "Kurchatov Institute," Moscow 123098, Russia  
<sup>35</sup>Kyoto University, Kyoto 606-8502, Japan  
<sup>36</sup>Laboratoire Leprince-Ringuet, Ecole Polytechnique, CNRS-IN2P3, Route de Saclay, F-91128 Palaiseau, France  
<sup>37</sup>Physics Department, Lahore University of Management Sciences, Lahore 54792, Pakistan  
<sup>38</sup>Lawrence Livermore National Laboratory, Livermore, California 94550, USA  
<sup>39</sup>Los Alamos National Laboratory, Los Alamos, New Mexico 87545, USA  
<sup>40</sup>LPC, Université Blaise Pascal, CNRS-IN2P3, Clermont-Fd, 63177 Aubiere Cedex, France  
<sup>41</sup>Department of Physics, Lund University, Box 118, SE-221 00 Lund, Sweden  
<sup>42</sup>University of Maryland, College Park, Maryland 20742, USA  
<sup>43</sup>Department of Physics, University of Massachusetts, Amherst, Massachusetts 01003-9337, USA  
<sup>44</sup>Department of Physics, University of Michigan, Ann Arbor, Michigan 48109-1040, USA  
<sup>45</sup>Institut für Kernphysik, University of Muenster, D-48149 Muenster, Germany  
<sup>46</sup>Muhlenberg College, Allentown, Pennsylvania 18104-5586, USA  
<sup>47</sup>Myongji University, Yongin, Kyonggido 449-728, Korea  
<sup>48</sup>Nagasaki Institute of Applied Science, Nagasaki-shi, Nagasaki 851-0193, Japan  
<sup>49</sup>University of New Mexico, Albuquerque, New Mexico 87131, USA  
<sup>50</sup>New Mexico State University, Las Cruces, New Mexico 88003, USA  
<sup>51</sup>Department of Physics and Astronomy, Ohio University, Athens, Ohio 45701, USA  
<sup>52</sup>Oak Ridge National Laboratory, Oak Ridge, Tennessee 37831, USA  
<sup>53</sup>IPN-Orsay, Université Paris Sud, CNRS-IN2P3, BP1, F-91406 Orsay, France

<sup>54</sup>*Peking University, Beijing 100871, People's Republic of China*<sup>55</sup>*PNPI, Petersburg Nuclear Physics Institute, Gatchina, Leningrad Region 188300, Russia*<sup>56</sup>*RIKEN Nishina Center for Accelerator-Based Science, Wako, Saitama 351-0198, Japan*<sup>57</sup>*RIKEN BNL Research Center, Brookhaven National Laboratory, Upton, New York 11973-5000, USA*<sup>58</sup>*Physics Department, Rikkyo University, 3-34-1 Nishi-Ikebukuro, Toshima, Tokyo 171-8501, Japan*<sup>59</sup>*Saint Petersburg State Polytechnic University, St. Petersburg 195251, Russia*<sup>60</sup>*Universidade de São Paulo, Instituto de Física, Caixa Postal 66318, São Paulo CEP05315-970, Brazil*<sup>61</sup>*Seoul National University, Seoul 151-742, Korea*<sup>62</sup>*Chemistry Department, Stony Brook University, SUNY, Stony Brook, New York 11794-3400, USA*<sup>63</sup>*Department of Physics and Astronomy, Stony Brook University, SUNY, Stony Brook, New York 11794-3400, USA*<sup>64</sup>*University of Tennessee, Knoxville, Tennessee 37996, USA*<sup>65</sup>*Department of Physics, Tokyo Institute of Technology, Oh-okayama, Meguro, Tokyo 152-8551, Japan*<sup>66</sup>*Institute of Physics, University of Tsukuba, Tsukuba, Ibaraki 305, Japan*<sup>67</sup>*Vanderbilt University, Nashville, Tennessee 37235, USA*<sup>68</sup>*Waseda University, Advanced Research Institute for Science and Engineering, 17 Kikui-cho, Shinjuku-ku, Tokyo 162-0044, Japan*<sup>69</sup>*Weizmann Institute, Rehovot 76100, Israel*<sup>70</sup>*Institute for Particle and Nuclear Physics, Wigner Research Centre for Physics, Hungarian Academy of Sciences (Wigner RCP, RMKI) H-1525 Budapest 114, P.O. Box 49, Budapest, Hungary*<sup>71</sup>*Yonsei University, IPAP, Seoul 120-749, Korea*

(Received 10 February 2014; published 3 June 2014)

Charged-pion-interferometry measurements were made with respect to the second- and third-order event plane for Au + Au collisions at  $\sqrt{s_{NN}} = 200$  GeV. A strong azimuthal-angle dependence of the extracted Gaussian-source radii was observed with respect to both the second- and third-order event planes. The results for the second-order dependence indicate that the initial eccentricity is reduced during the medium evolution, which is consistent with previous results. In contrast, the results for the third-order dependence indicate that the initial triangular shape is significantly reduced and potentially reversed by the end of the medium evolution, and that the third-order oscillations are largely dominated by the dynamical effects from triangular flow.

DOI: 10.1103/PhysRevLett.112.222301

PACS numbers: 25.75.Dw

The quark-gluon plasma (QGP), a state of nuclear matter in which quarks and gluons are deconfined, is produced in nuclear collisions at sufficiently high energy [1–4]. Once formed, the QGP expands, cools, and then freezes out into a collection of final-state particles. From extensive measurements of final-particle momenta and correlations, a detailed space-time picture of the evolution of the QGP is emerging [5,6], but detailed studies of the final space-time distribution of hadrons and an understanding of the dependence on the initial-collision geometry are needed to complete this picture.

Quantum-statistical interferometry of two identical particles, also known as Hanbury Brown–Twiss (HBT) interferometry [7,8], provides information on the space-time extent of the particle-emitting source. In heavy-ion collisions, hadron interferometry is sensitive to the space-time extent of the hadronic system at the time of the last scattering, referred to as kinetic freeze-out. In noncentral collisions of like nuclei, the initial density distribution is predominantly elliptical in shape, with additional fluctuations [9]. There is a larger pressure gradient along the minor axis (in plane) of the ellipse, compared to that along the major axis (out of plane), and this leads to a stronger expansion of the source within the in-plane direction. This phenomenon, elliptic flow, reduces the eccentricity of the

spatial distribution in the transverse plane, and may even reverse the major and minor axes of the initial distributions. Previous results are consistent with the picture that the final distribution still retains the initial elliptical orientation, although with a smaller eccentricity upon freeze-out [10].

The full set of anisotropic moments of the flow is characterized by the Fourier coefficients of the azimuthal distribution of emitted particles:  $dN/d\phi \propto 1 + 2 \sum v_n \cos[n(\phi - \Psi_n)]$ , where  $\phi$  is the azimuthal angle of the particle,  $v_n$  is the strength of  $n$ th-order flow harmonic, and  $\Psi_n$  is the  $n$ th-order event plane, where  $\Psi_2$  and  $\Psi_3$  are independent [11]. Elliptic flow is defined by the second-order coefficient ( $n = 2$ ), but triangular ( $n = 3$ ), quadrangular ( $n = 4$ ), and higher-order moments are also present and have been measured in both the spatial and momentum distributions in heavy-ion collisions [11–13]. While the higher-order even moments are needed to accurately describe the original elliptic shape, the odd moments arise predominantly through fluctuations in the initial spatial distribution or parity-odd processes, which are presumably small. Depending on strength of the fluctuations, flow profile, expansion time, and shear viscosity, these initial spatial fluctuations may be preserved until freeze-out [14,15].

In relativistic heavy-ion collisions, HBT interferometry with respect to different order event planes uniquely probes the magnitude of the initial-state fluctuations and the subsequent space-time evolution, thereby providing important constraints on the dynamics of the QGP. Here, we present results of azimuthal HBT measurements of charged pions with respect to the second-order event plane, as well as the first results with respect to the third-order event plane in Au + Au collisions at  $\sqrt{s_{NN}} = 200$  GeV at central rapidity. The centrality and transverse momentum dependence are also presented.

This analysis is based on data collected in 2007 with the PHENIX detector [16]. Collision centrality was determined using the measured charge distribution in the beam-beam counters ( $3.0 < |\eta| < 3.9$ ) [17]. The event planes  $\Psi_n$  were determined using the reaction plane detector (RXNP) covering forward and backward angles  $1.0 < |\eta| < 2.8$  [18]. The event plane resolution  $\text{res}(\Psi_n)$  was estimated by the two-subevent method [19] using the  $\Psi_n$  correlation between the RXNP at forward and backward angles, where  $\text{res}(\Psi_n)$  is defined as  $\langle \cos[n(\Psi_n - \Psi_{n,\text{real}})] \rangle$ . Track and momentum reconstruction of charged particles was performed by combining hits from the drift chamber and pad chambers in the central spectrometers ( $|\eta| < 0.35$ ), where the momentum resolution is  $\delta p/p \approx 1.3\% \oplus 1.2\% \times p$  [20]. Charged pions were identified by combining time of flight from the electromagnetic calorimeters [21] covering azimuthal angle  $\Delta\phi = \pi/2$ , with reconstructed momentum and trajectory in the magnetic field. Particles within 2 standard deviations of the peak of charged pions in mass-squared distributions were identified as pions up to a momentum of  $\sim 1$  GeV/c.

The experimentally measured correlation function is defined as  $A(q)/B(q)$ , where  $A(q)$  is the relative-momentum distribution of all combinations of identified pion pairs in the same event, and  $B(q)$  is the event-mixed background distribution of pairs formed from pions from different events, but with similar event centralities, vertex positions, and second-order (third-order) event planes. To remove ghost tracks and detector inefficiencies, pairs with either  $\Delta z < 5$  cm and  $\Delta\phi < 0.07$  or  $\Delta z < 70$  cm and  $\Delta\phi < 0.02$  at the drift chamber were removed from the analysis, as were tracks separated by less than 17 cm at the front face of the electromagnetic calorimeters. The correlation functions were also binned according to the centrality of the event and the momentum of the pion pair. Positive and negative pion pairs were combined to cancel charge-dependent acceptance effect [22].

A three-dimensional analysis was performed with the Bertsch-Pratt parametrization assuming a Gaussian source [23,24],

$$G = \exp(-R_s^2 q_s^2 - R_o^2 q_o^2 - R_l^2 q_l^2 - 2R_{os}^2 q_s q_o). \quad (1)$$

In this framework, the relative momentum  $\mathbf{q}$  is decomposed into  $q_l$ ,  $q_o$ , and  $q_s$ , where  $q_l$  denotes the beam direction,  $q_o$

is perpendicular to  $q_l$  and parallel to the mean transverse momentum of the pair  $\bar{k}_T = (\bar{p}_{1T} + \bar{p}_{2T})/2$ , and  $q_s$  is perpendicular to both  $q_l$  and  $q_o$ . The  $R_\mu$  ( $\mu = s, o, l$ ) Gaussian parameters provide information on the size of the emission region in each direction, but  $R_o$  and (to a lesser extent)  $R_l$  include contributions from the emission duration and all are influenced by position-momentum correlations. The  $R_{os}$  is a cross term that arises from asymmetries in the emission region [25]. The analysis was performed in the longitudinally comoving system, where  $p_{1z} = -p_{2z}$ . The measured correlation functions were fit by

$$C_2 = N\{\lambda(1+G)F_c + (1-\lambda)\}, \quad (2)$$

where  $N$  is a normalization factor and  $F_c$  is the Coulomb correction factor evaluated using a Coulomb wave function [22,26]. Equation (2) is based on the core-halo model [27,28], which divides the source into two regions: a central core that contributes to the quantum interference and a long-range component that includes the decay of long-lived particles having a negligible Coulomb interaction and a quantum statistical interference that occurs in a relative momentum range that is too small to be resolved experimentally. The fraction of pairs in the core is given by  $\lambda$ .

Finite event-plane resolution reduces the oscillation amplitude of HBT radii relative to the event plane. In this analysis, a model-independent correction suggested in Ref. [29] was applied to  $A(q)$  and  $B(q)$ . The correction factor is 54% (32%) for the second-order (third-order) event planes in 0%–10% centrality. As a cross-check, the oscillation amplitude was also corrected by dividing by  $\text{res}(\Psi_n)$  [30]. Both methods applied to the second- and third-order event-plane dependence are consistent within systematic uncertainties. The effect of momentum resolution was studied using GEANT simulations following previous analyses [22,31] and its impact is negligible on the extracted radii ( $< 1\%$ ).

Systematic uncertainties were estimated by the variation of single track cuts, pair selection cuts, and input source size for the Coulomb wave function. Also incorporated were the variations when using alternate event-plane definitions from the forward, backward, and combined RXNPs. Total systematic uncertainties for  $R_s^2$  and  $R_o^2$  are not more than 5% (12%) and 7% (17%) for the second-order (third-order) event plane, respectively.

Figure 1 shows  $R_s^2$ ,  $R_o^2$ ,  $R_l^2$ , and  $R_{os}^2$  for pions as functions of azimuthal angle  $\phi$  with respect to  $\Psi_2$  and  $\Psi_3$  for two centrality bins, where  $\langle k_T \rangle \approx 0.53$  GeV/c. The filled symbols show the extracted HBT radii and the open symbols are reflected by symmetry around  $\phi - \Psi_n = 0$ . For the 0%–10% bin,  $R_s^2$  shows a very weak oscillation relative to both  $\Psi_2$  and  $\Psi_3$ , while  $R_o^2$  clearly exhibits a stronger oscillation. For the 20%–30% bin,  $R_s^2$  and  $R_o^2$  for  $\Psi_2$  show opposite-sign oscillations, as expected for an elliptical source viewed from in-plane and out-of-plane axes [10]. For  $\Psi_3$ ,  $R_s^2$  shows a weaker angular dependence of the same sign as  $R_o^2$ .

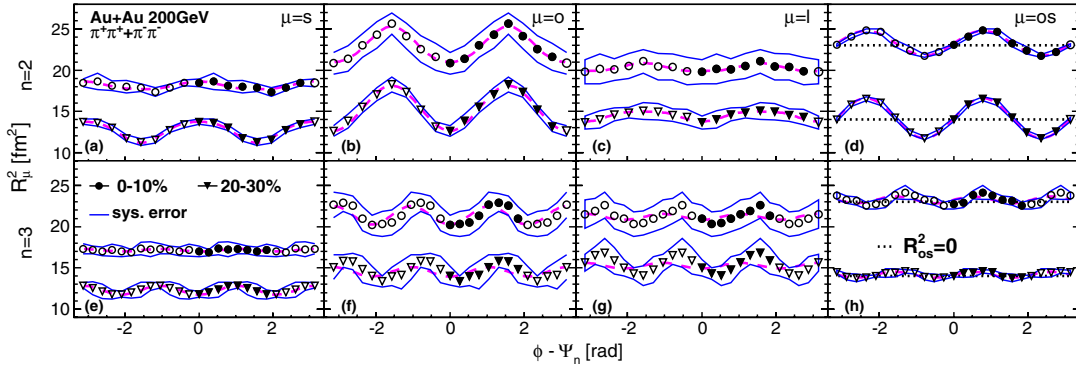


FIG. 1 (color online). The azimuthal dependence of  $R_s^2$ ,  $R_o^2$ ,  $R_l^2$ , and  $R_{os}^2$  for charged pions in  $0.2 < k_T < 2.0$  GeV/ $c$  with respect to second-(a)–(d) and third-order (e)–(h) event plane in Au + Au collisions at  $\sqrt{s_{NN}} = 200$  GeV. The  $R_{os}^2$  is plotted relative to dotted lines representing  $R_{os}^2 = 0$ . The filled symbols show the extracted HBT radii and the open symbols are reflected by symmetry around  $\phi - \Psi_n = 0$ . Bands of two thin lines show the systematic uncertainties and dashed lines show the fit lines by Eq. (3).

The oscillation amplitudes were extracted by fitting the angular dependence of  $R_\mu^2$  to the functional form,

$$R_\mu^2 = R_{\mu,0}^2 + 2 \sum_{n=m,2m} R_{\mu,n}^2 \cos[n(\phi - \Psi_m)] \quad (\mu = s, o, l),$$

$$R_\mu^2 = 2 \sum_{n=m,2m} R_{\mu,n}^2 \sin[n(\phi - \Psi_m)] \quad (\mu = os), \quad (3)$$

where  $R_{\mu,n}^2$  are the Fourier coefficients [32].

Figure 2 shows the amplitudes relative to the average of  $R_s^2$ ,  $R_o^2$ , and  $R_{os}^2$ ,  $2R_{\mu,n}^2/R_{\nu,0}^2$ , as functions of initial eccentricity ( $\epsilon_2$ ) and triangularity ( $\epsilon_3$ ). Each  $\epsilon_n$  is calculated by Monte Carlo Glauber simulation as given in Refs. [15,33]

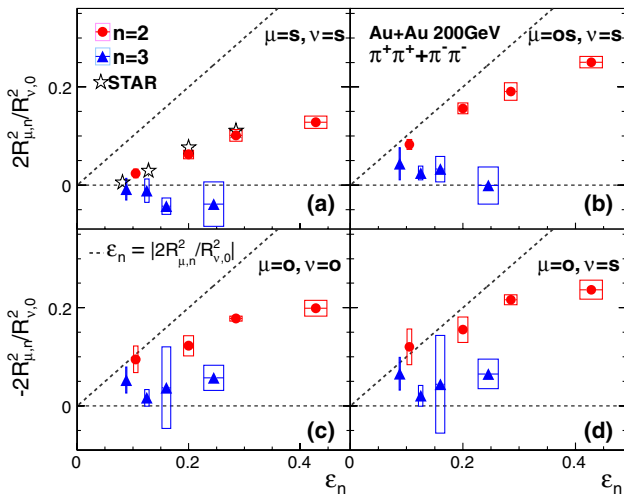


FIG. 2 (color online). The solid points are the oscillation amplitudes relative to the average of HBT radii for four different combinations (a)  $2R_{s,n}^2/R_{s,0}^2$ , (b)  $2R_{os,n}^2/R_{s,0}^2$ , (c)  $2R_{o,n}^2/R_{o,0}^2$ , and (d)  $2R_{o,n}^2/R_{s,0}^2$ , as a function of initial spatial anisotropy ( $\epsilon_n$ ), which are calculated using the Glauber model. Boxes show the systematic uncertainties. Open star symbols are the  $\epsilon_{\text{final}}$  from STAR [10]. Dashed lines indicate the line of  $\epsilon_n = |2R_{\mu,n}^2/R_{\nu,0}^2|$ .

and decreases with increasing centrality; however, the centrality dependence of  $\epsilon_3$  is weaker than that of  $\epsilon_2$ .

The  $2R_{s,2}^2/R_{s,0}^2$  [Fig. 2(a)] is sensitive to the final source eccentricity ( $\epsilon_{\text{final}}$ ) at freeze-out [29], and approaches the whole source eccentricity in the limit of  $k_T = 0$ . Our results for the  $\Psi_2$  dependence are consistent with the STAR experiment [10]. We note that the  $\epsilon_{\text{final}}$  defined from  $R_s$  has a systematic uncertainty of 30% due to the assumption of space-momentum correlation in the blast-wave model [29]. The positive value of  $\epsilon_{\text{final}}$  indicates that the source shape still retains the initial shape extended out of plane, though reduced in magnitude. Other combinations of  $|2R_{\mu,2}^2/R_{\nu,0}^2|$  also have similar  $\epsilon_n$  dependence, but are larger than  $2R_{s,2}^2/R_{s,0}^2$ . They include contributions from the emission duration and will have different sensitivity to the dynamics [34]. The  $2R_{s,3}^2/R_{s,0}^2$  are less than or equal to zero, which seems to be an opposite trend to other combinations, as noted already in Fig. 1. For all amplitudes, the values for third order are small compared to those for second order.

It is well known that the HBT radii are influenced by the presence of dynamical correlations between momentum and spatial distributions at the time of freeze-out [35,36], as evident in the transverse pair momentum  $k_T$  dependence of the radii. Figure 3 shows these results for the third-order oscillation amplitudes. The  $R_{o,3}^2/R_{o,0}^2$  decreases with  $k_T$ , whereas  $R_{s,3}^2/R_{s,0}^2$  does not show a significant dependence.

Although the reduced third-order anisotropy in Fig. 3 may indicate small triangular deformation at freeze-out, its interpretation is complicated by the influence of dynamical correlations from the triangular flow [40]. To illustrate the different contributions of these effects, we show separately the  $k_T$  dependence for a source with radial symmetry and triangular flow ( $\bar{\epsilon}_3 = 0$ ,  $\bar{v}_3 = 0.25$ ) and a source with triangular deformation and radial flow ( $\bar{\epsilon}_3 = 0.25$ ,  $\bar{v}_3 = 0$ ) [37]. The model curves are taken from Ref. [40], but the radii are scaled by 0.3 to fit within the

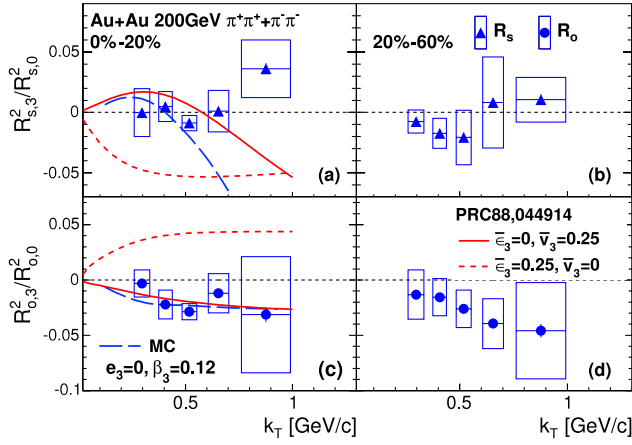


FIG. 3 (color online).  $k_T$  dependence of  $R_s^2$  [(a),(b)] and  $R_o^2$  [(c),(d)] amplitudes relative to their averages for the third-order event plane in two centrality bins. Calculations of the Gaussian source model [40] are shown as solid and short-dashed (red) curves, where the values are scaled by 0.3. Calculations using the Monte Carlo simulation are shown as long-dashed (blue) curves.

range of the data. The  $R_{o,3}^2$  favors the deformed flow scenario, while the  $R_{s,3}^2$  matches the deformed flow only at lower  $k_T$ .

To disentangle the relative contributions of spatial and flow anisotropy to the azimuthal dependence of HBT radii, we have performed a Monte Carlo simulation introducing the spatial anisotropy and collective flow with anisotropic modulation at freeze-out. The assumptions of this model are similar to those adopted in the blast-wave model [29,38], generalized for third-order modulation, and do not include effects such as viscosity and source opacity. The particle distributions in the transverse plane were parametrized with a Woods-Saxon function,  $\Omega(r) = 1/\{1 + \exp[(r-R)/a]\}$ . To control the final source triangularity, we introduced a parameter  $e_3$  into the radius parameter  $R$  in  $\Omega(r)$  as follows:

$$R = R_0\{1 - 2e_3 \cos[3(\phi - \Phi)]\}, \quad (4)$$

$$\beta_T = \beta_0\{1 + 2\beta_3 \cos[3(\phi - \Phi)]\}, \quad (5)$$

where  $\phi$  is the azimuthal angle of particle positions,  $\Phi$  is the reference angle of the spatial anisotropy and triangular flow, and  $R_0$  is the average radius. To take the collective flow into account, generated particles were boosted in the transverse radial direction with a velocity  $\beta_T$  in addition to their thermal velocities. We used a similar definition to the blast-wave model [29,38] as the flow rapidity  $\rho(r) = (r/R)\tanh^{-1}(\beta_T)$ . In Eq. (5),  $\beta_0$  represents the average of radial flow and  $\beta_3$  is used to control the flow anisotropy. We assume that the particles are emitted with a Gaussian time distribution with  $\Delta\tau$  standard deviation, which affects  $R_o$  but not  $R_s$ . The effect of HBT interference was calculated by  $\cos(\Delta\mathbf{x} \cdot \mathbf{q})$ , where  $\Delta\mathbf{x}$  and  $\mathbf{q}$  are

4-vectors for relative distance and relative momentum of the pair. All other parameters except  $e_3$  and  $\beta_3$  were tuned to reproduce the strength of radial flow measured by  $m_T$  spectra [39] and the averages of HBT radii shown in Fig. 1. For this analysis  $\Delta\tau$  was set to 3.5 fm/c (2.7 fm/c) for 0%–10% (20%–30%) to achieve better agreement with the average of  $R_o^2$ . A simulation result with  $e_3 = 0$  and  $\beta_3 = 0.12$  is shown in Fig. 3, displaying a trend that is qualitatively consistent with Ref. [40].

To understand how the data may constrain these values, we have performed a least-squares fit for  $e_3$  and  $\beta_3$ . Figure 4 shows the contour plots of  $\chi^2$  defined by  $\{([2R_{\mu,3}^2/R_{\mu,0}^2]^{\text{exp}} - [2R_{\mu,3}^2/R_{\mu,0}^2]^{\text{sim}})/E\}^2$ , where  $E$  is the experimental uncertainty. The value of  $e_3$  is well constrained by the measured value of  $R_s^2$ , and indicates that the final triangularity is very close to zero. The inclusion of  $R_o^2$  favors a positive value for  $\beta_3$  for 0%–10%, but does not add much information to 20%–30%, where a slightly negative value of  $e_3$  is favored by  $R_s^2$ . We note that the discrepancy at high  $k_T$  remains, but the data integrated over  $k_T$  are primarily influenced by lower  $k_T$  pairs. Detailed comparison with a realistic hydrodynamic model (e.g., Refs. [40,41]) will be a key to fully understanding the results.

In summary, we have presented results on the azimuthal dependence of charged-pion HBT radii with respect to second- and third-order event planes in Au + Au collisions at  $\sqrt{s_{NN}} = 200$  GeV. The results for the second-order event-plane dependence indicate that in noncentral events the source starts with an initial elliptical distribution and ends with an elliptical distribution at freeze-out, but with a diluted eccentricity due to the medium expansion. For the third-order event-plane results, the observed  $R_o^2$  oscillation may come from flow anisotropy, but the small  $R_s^2$  oscillation with the same sign as  $R_o^2$  in noncentral collisions may imply that the source expansion with triangular flow inverts the initial triangular shape. A Monte Carlo simulation for an expanding triangular transverse distribution produced results consistent with this interpretation. Comparisons

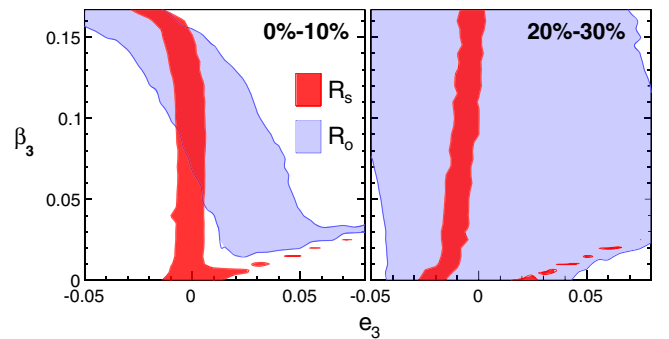


FIG. 4 (color online).  $\chi^2$  contours representing the difference between data and simulation in  $2R_{\mu,2}^2/R_{\mu,0}^2$  ( $\mu = s, o$ ), as functions of  $e_3$  and  $\beta_3$ . Shaded areas represent  $\chi^2$  less than unity and constrained by the experimental uncertainty.

with an event-by-event hydrodynamic model will be needed to reveal the relation of spatial and hydrodynamical flow anisotropy at freeze-out, as well as to provide further constraints on the hydrodynamic evolution in relativistic heavy-ion collisions.

We thank the staff of the Collider-Accelerator and Physics Departments at Brookhaven National Laboratory and the staff of the other PHENIX participating institutions for their vital contributions. We acknowledge support from the Office of Nuclear Physics in the Office of Science of the Department of Energy, the National Science Foundation, Abilene Christian University Research Council, Research Foundation of SUNY, and Dean of the College of Arts and Sciences, Vanderbilt University (U.S.); Ministry of Education, Culture, Sports, Science, and Technology and the Japan Society for the Promotion of Science (Japan); Conselho Nacional de Desenvolvimento Científico e Tecnológico and Fundação de Amparo à Pesquisa do Estado de São Paulo (Brazil); Natural Science Foundation of China (People's Republic of China); Ministry of Education, Youth and Sports (Czech Republic); Centre National de la Recherche Scientifique, Commissariat à l'Énergie Atomique, and Institut National de Physique Nucléaire et de Physique des Particules (France); Bundesministerium für Bildung und Forschung, Deutscher Akademischer Austausch Dienst, and Alexander von Humboldt Stiftung (Germany); Hungarian National Science Fund, OTKA (Hungary); Department of Atomic Energy and Department of Science and Technology (India); Israel Science Foundation (Israel); National Research Foundation and WCU program of the Ministry Education Science and Technology (Korea); Physics Department, Lahore University of Management Sciences (Pakistan); Ministry of Education and Science, Russian Academy of Sciences, Federal Agency of Atomic Energy (Russia); VR and Wallenberg Foundation (Sweden); the U.S. Civilian Research and Development Foundation for the Independent States of the Former Soviet Union, the U.S.-Hungarian Fulbright Foundation for Educational Exchange, and the U.S.-Israel Binational Science Foundation.

\*Deceased.

†PHENIX Co-Spokesperson.morrison@bnl.gov

\*PHENIX Co-Spokesperson.jamie.nagle@colorado.edu

- [1] K. Adcox *et al.* (PHENIX Collaboration), *Nucl. Phys.* **A757**, 184 (2005).
- [2] J. Adams *et al.* (STAR Collaboration), *Nucl. Phys.* **A757**, 102 (2005).
- [3] B. B. Back *et al.* (PHOBOS Collaboration), *Nucl. Phys.* **A757**, 28 (2005).
- [4] L. Arsene *et al.* (BRAHMS Collaboration), *Nucl. Phys.* **A757**, 1 (2005).

- [5] S. Pratt, *Phys. Rev. Lett.* **102**, 232301 (2009).
- [6] R. A. Soltz, I. Garishvili, M. Cheng, B. Abelev, A. Glenn, J. Newby, L. A. Linden Levy, and S. Pratt, *Phys. Rev. C* **87**, 044901 (2013).
- [7] R. H. Brown and R. Q. Twiss, *Nature (London)* **178**, 1046 (1956).
- [8] G. Goldhaber, S. Goldhaber, W. Lee, and A. Pais, *Phys. Rev.* **120**, 300 (1960).
- [9] U. Heinz and R. Snellings, *Annu. Rev. Nucl. Part. Sci.* **63**, 123 (2013).
- [10] J. Adams *et al.* (STAR Collaboration), *Phys. Rev. Lett.* **93**, 012301 (2004).
- [11] S. S. Adler *et al.* (PHENIX Collaboration), *Phys. Rev. Lett.* **107**, 252301 (2011).
- [12] K. Aamodt *et al.* (ALICE Collaboration), *Phys. Rev. Lett.* **107**, 032301 (2011).
- [13] G. Aad *et al.* (ATLAS Collaboration), *Phys. Rev. C* **86**, 014907 (2012).
- [14] S. A. Voloshin, *J. Phys. G* **38**, 124097 (2011).
- [15] B. Alver and G. Roland, *Phys. Rev. C* **81**, 054905 (2010).
- [16] K. Adcox *et al.* (PHENIX Collaboration), *Nucl. Instrum. Methods Phys. Res., Sect. A* **499**, 469 (2003).
- [17] M. Allen *et al.* (PHENIX Collaboration), *Nucl. Instrum. Methods Phys. Res., Sect. A* **499**, 549 (2003).
- [18] E. Richardson *et al.* (PHENIX Collaboration), *Nucl. Instrum. Methods Phys. Res., Sect. A* **636**, 99 (2011).
- [19] A. M. Poskanzer and S. A. Voloshin, *Phys. Rev. C* **58**, 1671 (1998).
- [20] A. Adare *et al.* (PHENIX Collaboration), *Phys. Rev. C* **85**, 064914 (2012).
- [21] L. Aphecetche *et al.* (PHENIX Collaboration), *Nucl. Instrum. Methods Phys. Res., Sect. A* **499**, 521 (2003).
- [22] J. Adams *et al.* (STAR Collaboration), *Phys. Rev. C* **71**, 044906 (2005).
- [23] S. Pratt, *Phys. Rev. D* **33**, 72 (1986).
- [24] G. Bertsch, M. Gong, and M. Tohyama, *Phys. Rev. C* **37**, 1896 (1988).
- [25] M. Lisa, S. Pratt, R. Soltz, and U. Wiedemann, *Annu. Rev. Nucl. Part. Sci.* **55**, 357 (2005).
- [26] S. S. Adler *et al.* (PHENIX Collaboration), *Phys. Rev. Lett.* **93**, 152302 (2004).
- [27] M. G. Bowler, *Phys. Lett. B* **270**, 69 (1991).
- [28] Yu. M. Sinyukov, R. Lednicky, S. V. Akkelin, J. Pluta, and B. Erazmus, *Phys. Lett. B* **432**, 248 (1998).
- [29] F. Retière and M. A. Lisa, *Phys. Rev. C* **70**, 044907 (2004).
- [30] D. Adamová *et al.* (CERES Collaboration), *Phys. Rev. C* **78**, 064901 (2008).
- [31] C. Alt *et al.* (NA49 Collaboration), *Phys. Rev. C* **77**, 064908 (2008).
- [32] The  $R_{\mu,n}^2$  as a fitting parameter could be negative, which means a different phase of the cosine function.
- [33] M. L. Miller, K. Reygers, S. J. Sanders, and P. Steinberg, *Annu. Rev. Nucl. Part. Sci.* **57**, 205 (2007).
- [34] U. Heinz and P. F. Kolb, *Phys. Lett. B* **542**, 216 (2002).
- [35] Y. Hama and S. S. Padula, *Phys. Rev. D* **37**, 3237 (1988).
- [36] S. V. Akkelin and Y. M. Sinyukov, *Phys. Lett. B* **356**, 525 (1995).

- [37]  $\bar{\epsilon}_3$  parametrizes the triangular spatial source deformation and  $\bar{v}_3$  represents the strength of a triangular flow in the model of Ref. [40].
- [38] S. S. Adler *et al.* (PHENIX Collaboration), *Phys. Rev. C* **72**, 014903 (2005).
- [39] S. S. Adler *et al.* (PHENIX Collaboration), *Phys. Rev. C* **69**, 034909 (2004).
- [40] C. J. Plumberg, C. Shen, and U. Heinz, *Phys. Rev. C* **88**, 044914 (2013).
- [41] P. Bozek, *Phys. Rev. C* **89**, 044904 (2014).